

Article - Engineering, Technology and Techniques

# Day-Ahead Operational Planning of Isolated Microgrids Considering Over/Underestimation Costs for Solar and Wind Power Generation and Battery Degradation Costs

**Wagner Felipe Santana Souza**<sup>1\*</sup>  
https://orcid.org/0000-0001-8093-5735

**Roman Kuiava**<sup>1</sup>  
https://orcid.org/0000-0002-6110-6189

**Ádamo Henrique Rocha de Oliveira**<sup>1</sup>  
https://orcid.org/0000-0002-5709-7857

**Gideon Villar Leandro**<sup>1</sup>  
https://orcid.org/0000-0002-2093-4551

**Carla Eduarda Orlando de Moraes de Lara**<sup>2</sup>  
https://orcid.org/0009-0006-0888-8819

<sup>1</sup>Universidade Federal do Paraná (UFPR), Departamento de Engenharia Elétrica, Curitiba, Brasil; <sup>2</sup>Centro Universitário Internacional (UNINTER), Departamento de Engenharia Elétrica, Curitiba, Brasil.

Editor-in-Chief: Alexandre Rasi Aoki  
Associate Editor: Daniel Navarro Gevers

Received: 24-Oct-2023; Accepted: 17-Sep-2024

\*Correspondence: wagnerfelipe@ufpr.br; Tel.: +5573991092961 (W.F.S.S.).

## HIGHLIGHTS

- Mathematical models referring to the energy resources available in the microgrid.
- Mathematical formulation of the Day-ahead operational planning.
- Tests and results for the proposed formulation applied in the considered microgrid.

**Abstract:** This paper proposes a methodology for the day-ahead operational planning of isolated microgrids equipped with renewable distributed generation based on solar photovoltaic and wind generation systems, energy storage systems, and diesel generation as backup power sources. As one of the main contributions of this paper, the proposed methodology is based on optimal power flow (OPF), considering cost minimization as the objective function that combines probabilistic costs of the renewable distributed generation systems with the determinist cost associated with the degradation of the battery bank. In addition, the cost of fuel consumption associated with the diesel generator is also considered. The costs associated with the renewable distributed generation are modeled by probability density functions, where a reserve cost for overestimation and a penalty cost for underestimation of the output power from these renewable sources are adopted. Hence, the proposed OPF avoids the over/underestimation of the available day-ahead solar and wind generations. The differential evolution optimization technique was used to solve the proposed OPF formulation and to obtain a minimum cost of operation considering the deterministic load profile for the operation of the microgrid under study. The proposed formulation was tested for different solar photovoltaic and wind generation scenarios in a microgrid in Lençóis Island, Brazil, another important contribution of the paper. The obtained results showed that the considered microgrid's day-ahead planning is sensitive to climatic conditions that impact the generation scenario and minimize long-term operating costs.

**Keywords:** Optimal Power Flow; Renewable Resources; Day-Ahead Operational Planning.

---

## INTRODUCTION

Isolated or standalone microgrids can be defined as low or medium-voltage electrical networks consisting of distributed generation based on renewable and non-renewable sources, energy storage devices, and controllable loads, operating disconnected from the main power grid [1]. The isolated microgrids are adopted to supply electrical energy in remote or difficult access areas, in which the supply of electric energy through the conventional network is unfeasible, either for political reasons or even due to the high cost of electricity generation and transmission.

In order to guarantee a sustainable operation of an isolated microgrid, the operating costs associated with the electrical energy production must be minimized, while the energy storage system lifetime is expected to be prolonged. However, due to the intermittent nature of some of these sources, the uncertainty related to power generation through renewable resources is one of the biggest challenges associated with the dimensioning, operation, and energy planning of isolated microgrids.

Day-ahead operational planning (DA-OP) in isolated microgrids consists of determining the daily operating conditions of the distributed generation units (in terms of dispatched active power) and the power generated (or consumed) by the energy storage system for a forecasted load demand during a scheduling period, normally defined as the 24 hours of the following day, discretized at 24 operating points [2]. The operating costs of these isolated microgrids can be minimized using optimal power flow (OPF) formulated in the context of day-ahead operational planning [3].

In addition to (DA-OP), the application of OPF to real-time power dispatch (RT-PD) has been widely discussed [4, 5]. The main difference between these two strands of OPF application is the considered scheduling time horizon. While in the DA-OP the power values are obtained for each hour of the next day, the RT-PD determines the power dispatch of each generating unit and the operating conditions of the storage system at intervals of 5 to 15 minutes ahead of the current time. The practical effects of this temporal difference between the DA-OP and RT-PD can be observed in the value of the power dispatch in microgrids containing wind turbines and photovoltaic panels. The presence of intermittent energy sources significantly implies the day-ahead planning, since solar irradiance and wind speed values are sensitive to medium-term forecasts (in case, from one to a few days) [6].

Several papers propose the use of DA-OP for microgrids. In [2], for example, a DA-OP is combined with a RT-PD in a microgrid with generation based on intermittent renewable sources. Also, a deterministic approach was adopted to describe the solar irradiance and wind speed profiles. This approach usually provides satisfactory results for real-time dispatch, however, the same performance is not guaranteed for the DA-OP, since power variations in renewable generation were not considered in the proposed formulation. In this context, [7] proposed a DA-OP formulation considering the intermittent nature of solar and wind energy. Nevertheless, it is important to emphasize that energy storage systems are not considered in papers both [2] and [7], which is a simplification that reduces the complexity of day-ahead planning in isolated microgrids.

Regarding operational planning of microgrids with energy storage systems, [8] and [9] propose a DA-OP that maximizes the lifetime of lead-acid batteries by modeling the battery aging process and minimizing the costs of the microgrid in long-term operation. These papers present interesting results for day-ahead operational planning, once the global optimal point is obtained. However, these papers neglect the uncertainties related to renewable generation, which may lead to results far from reality.

Recent papers have been looking for alternatives to deal with the uncertainties associated with intermittent resources. Paper [10], for example, proposes a stochastic optimization for DA-OP with security constraints under photovoltaic production uncertainties. The purpose of planning is to minimize carbon dioxide emissions and operating costs. Also, paper [11] proposes a framework for the DA-OP, which considers the uncertainties using a robust optimization approach where the obtained results demonstrate the importance of considering the uncertainties associated with intermittent resources. In the same way, [12] and [13] formulate a DA-OP that considers the aging process of the battery bank and present the stochasticity of the intermittent renewable sources. However, in papers [10-13], wind generation is not considered in the studied microgrid, which is a very common energy resource in isolated microgrids [14].

Paper [15] proposes a RT-PD strategy based on the results obtained from the DA-OP to adjust the real-time operational planning by considering the actual values of the load and renewable energy generation. These considerations have a direct impact on the economy of the system, however, the considered microgrid is connected to the main distribution network, which differs from the approach addressed in this paper.

The previously discussed papers [7-13,15] do not consider the optimization of the energy storage system lifetime, concurrently with a probabilistic cost model for the distributed generation based on intermittent resources, which represents a gap to be filled by this paper. In this context, this paper proposes a DA-OP for a microgrid operating in standalone mode and equipped with solar and wind generation, as well as a diesel generator and a battery bank. Since the main generation of the considered microgrid is based on intermittent sources, it is extremely important to consider costs models that takes into account the intermittent nature of these sources, to avoid an overestimated or underestimated operational planning results in terms of their power dispatch. Furthermore, a very harsh operating regime may be imposed to the battery bank due to the intermittent nature of intermittent sources. Considering these storage systems represent a significant portion of the total cost of the microgrid, operation strategies that preserve its useful life become very attractive.

As the main contribution of this paper, the proposed DA-OP formulation considers the degradation of the battery bank and the intermittent nature inherent to solar photovoltaic systems (PVS) and wind generation systems (WGS). These considerations are important, as they promote the optimization of the battery's useful life, better energy use from intermittent sources, and the reduction of microgrid operating costs in the long term. In this formulation, the objective function combines the probabilistic costs of the PVS and WGS with the determinist costs of both the conventional diesel generator and the battery bank. Also, the proposed DA-OP aims to avoid the overestimation and underestimation of the available day-ahead solar and wind generations by considering in the objective function a reserve cost for overestimation and a penalty cost for underestimation of the output power from these renewable sources. The proposed DA-OP is solved by Differential Evolution (DE) algorithm [16]. Another important contribution of the paper is the adoption of a real isolated microgrid as a test system, which is located in Lençóis Island, Brazil.

## ENERGY RESOURCES IN ISOLATED MICROGRIDS

Microgrids operating in standalone mode are usually equipped with renewable resources and energy storage systems, in addition to a power backup given by diesel generators, which are used to increase the reliability of the system. Figure 1 presents the structure of the microgrid considered in this paper and the signal convention scheme adopted for the active power flow.

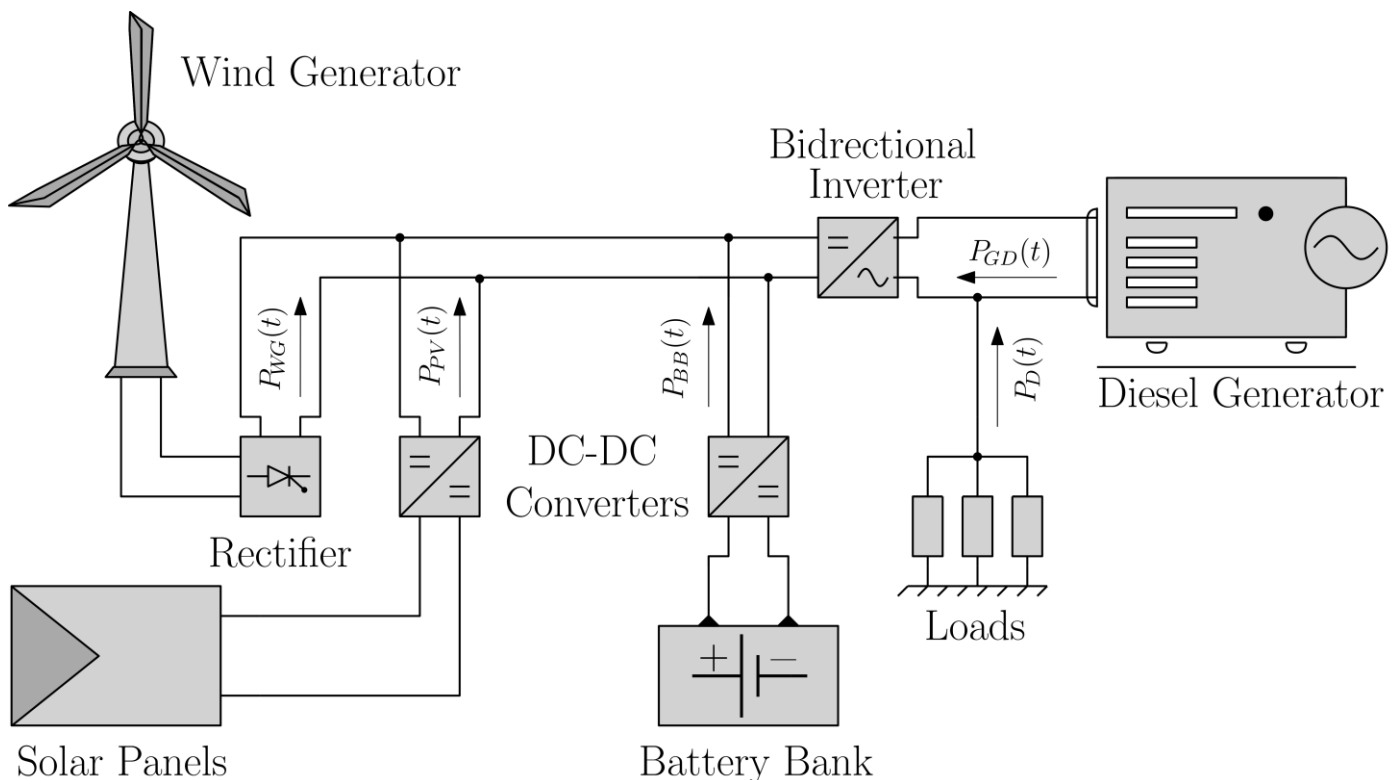


**Figure 1.** Structure of the microgrid and the adopted signal convention.

In the next subsections, the mathematical models referring to the energy resources presented in Figure 1 are presented.

## Probabilistic Cost Model for Solar Photovoltaic and Wind Generation

The model of the cost associated with solar and wind generation is based on the uncertainties related to the availability of active power from these resources. In the next subsections, the probabilistic modeling of the available power of intermittent generation resources is presented, so that the probabilistic cost model for solar and wind generation is presented.

### Probabilistic Model of the Solar Photovoltaic Generation System

This subsection presents a probabilistic model for the available power in a PVS. As shown in [17,18] this available power is a function of the clearness index,  $k_t$ , which is defined by the relation  $I_t/I_o$ , where  $I_t$  is the terrestrial surface and  $I_o$  is the irradiance measured outside the atmosphere. Furthermore, considering that a PVS is equipped with a maximum power point tracker (MPPT), the relationship between the generated power,  $P_{PV}(t)$ , in kW, and the hourly clearness index,  $k_t(t)$ , is given by [19]:

$$P_{PV}(k_t, t) = A_c \eta \left( T(t) k_t(t) - T'(t) k_t^2(t) \right) \quad (1)$$

where  $t = 1, 2, \dots, 24$  is the hourly time,  $A_c$  is the PVS panels area ( $m^2$ ) and  $\eta$  is the efficiency of the PVS (including the efficiency of the inverters). Also,  $T(t)$  and  $T'(t)$  are parameters that depend on local characteristics of the PVS, such as latitude and longitude coordinates, inclination of PVS panels and others [20]. Moreover,  $k_t(t)$  is a random variable with a known probability density function (PDF) [21]. So, using the fundamental random variable theorem [15], it is possible to obtain the PDF for the active power output available in the PVS,  $f_{P_{PV}}(P_{PV}(k_t, t))$ , which is given by:

$$f_{P_{PV}}(P_{PV}(k_t, t)) = \begin{cases} \frac{c(k_{tu} - \frac{1}{2}(\alpha(t) + \alpha'(t)))}{-k_{tu} A_c \eta T'(t) \alpha'(t)} e^{\frac{\lambda}{2}(\alpha(t) + \alpha'(t))} & \text{if } P_{PV} \in [0, P_{PV}(k_{tu}, t)] \\ 0 & \text{otherwise} \end{cases} \quad (2)$$

for  $T(t) > 0$  and  $T'(t) < 0$ , and

$$f_{P_{PV}}(P_{PV}(k_t, t)) = \begin{cases} \frac{c(k_{tu} - \frac{1}{2}(\alpha(t) - \alpha'(t)))}{k_{tu} A_c \eta T'(t) \alpha'(t)} e^{\frac{\lambda}{2}(\alpha(t) - \alpha'(t))} & \text{if } P_{PV} \in [0, P_{PV}(k_{tu}, t)] \\ 0 & \text{otherwise} \end{cases} \quad (3)$$

for  $T(t) > 0$  and  $T'(t) \geq 0$ , where  $\alpha(t) = \frac{T(t)}{T'(t)}$  and  $\alpha'(t) = \sqrt{\alpha^2(t) - \frac{4P_{PV}(k_t, t)}{A_c \eta T'(t)}}$ . Also,  $P_{PV}(k_{tu}, t)$  is calculated by (1) where  $k_t$  is assumed to be equal to  $k_{tu}$ . Thus, the maximum available active power in the PVS,  $P_{PV}(k_{tu}, t)$ , at instant  $t$  is a function of the maximum clearness index,  $k_{tu}$ , at this same instant  $t$ . Equations (2) and (3) provide the PDF of the active power available in the PVS at time  $t$ .

### Probabilistic Model of the Wind Generation System (WGS)

This subsection presents a probabilistic model for the available power in a WGS. This available power is a function of the wind speed. Several functions can be used for this purpose, where each one represents a certain wind speed distribution [22]. However, a widely used and accepted distribution to represent the PDF of wind speed is the Weibull function [23, 24].

A probabilistic model of the available active power from a wind turbine can be determined by using the wind speed model given by the Weibull function [23]. In practice, wind turbines have physical limitations and are equipped with control systems that limit their maximum active power generated. Then, the relationship between the active power from a wind turbine,  $P_{WG}$  and the wind speed  $v$  is commonly approximated by a linear function [25, 26]. The relationship between  $P_{WG}$  and  $v$  is then given by:

$$P_{WG}(v, t) = \begin{cases} 0 & \text{if } 0 \leq v(t) \leq v_i \\ P_{WG}^R \left( \frac{v(t) - v_i}{v_r - v_i} \right) & \text{if } v_i \leq v(t) \leq v_r \\ P_{WG}^R & \text{if } v_r \leq v(t) \leq v_o \\ 0 & \text{if } v(t) \geq v_o \end{cases} \quad (4)$$

The PDF of the available active power of a WGS can be obtained by using the fundamental random variable theorem,  $f_{P_{WG}}(P_{WG}(v, t))$ , which is given by:

$$f_{P_{WG}}(P_{WG}(v, t)) = \begin{cases} 1 - \exp\left[-\left(\frac{v_i}{c}\right)^{k_v}\right] + \exp\left[-\left(\frac{v_o}{c}\right)^{k_v}\right] & \text{if } P_{WG}(v, t) = 0 \\ \left(\frac{k_v v_i}{c}\right) \left(\frac{(1+\rho l)v_i}{c}\right)^{k_v-1} \exp\left[-\left(\frac{(1+\rho l)v_i}{c}\right)^{k_v}\right] & \text{if } 0 < P_{WG}(v, t) < P_{WG}^R \\ -\exp\left[-\left(\frac{v_i}{c}\right)^{k_v}\right] + \exp\left[-\left(\frac{v_o}{c}\right)^{k_v}\right] & \text{if } P_{WG}(v, t) = P_{WG}^R \end{cases} \quad (5)$$

where,  $\rho = \frac{P_{WG}(v, t)}{P_{WG}^R}$ ,  $l = \frac{v_r - v_i}{v_i}$  and  $v_i$ ,  $v_r$  and  $v_o$  are the input shear speed, output shear speed and rated speed, of the wind turbine, respectively. Also,  $P_{WG}^R$  is the rated power of the wind turbine.

### Cost Model for PVS and WGS

The uncertainties on the generated active power of a PVS and WGS can be modeled by including an overestimation and underestimation penalties in the cost functions [27, 28]. Hence, the total generation cost associated with a wind and solar resource  $X$ , where  $X$  is a sub-index for wind and solar sources,  $X = \{PV, WG\}$ , can be described as:

$$F_x(P_{Xp}(t)) = C_X^l(P_{Xp}(t)) + C_X^p(P_{Xd}(t), P_{Xp}(t)) + C_X^r(P_{Xd}(t), P_{Xp}(t)) \quad (6)$$

where  $C_X^l$ ,  $C_X^p$  e  $C_X^r$  are the linear, underestimation and overestimation costs of the resource  $X$ , respectively.

Also,  $P_{Xp}(t)$  e  $P_{Xd}(t)$  are the planned and available active powers for the resource  $X$ , with the first one ( $P_{Xp}(t)$ ) being the OPF control variable and representing the amount of active power that must be supplied by the PVS and WGS to the microgrid at time  $t$ . Meanwhile,  $P_{Xd}(t)$  is the available active power, which is a variable with random behavior, ruled by the PDF associated with the power generation of the intermittent resource.

The first term of equation (6) represents a linear cost function, which can be associated to fixed expenses, such as the maintenance of the intermittent resource. Mathematically it can be determined as follows:

$$C_X^l(P_{Xp}(t)) = k_X^l P_{Xp}(t) \quad (7)$$

where  $k_X^l$  is the linear cost coefficient for the intermittent resource  $X$ .

The second term of equation (6) is the penalty cost, obtained from the concept of underestimation of the intermittent resource. It represents the cost charged for not using all the energy available in the PVS or WGS, that is [20,28]:

$$C_X^p(P_{Xd}(t), P_{Xp}(t)) = k_X^p \int_{P_{Xp}(t)}^{P_X^{max}(t)} (P_X(t) - P_{Xp}(t)) f_{P_X}(P_X(t)) dP_X(t) \quad (8)$$

where  $k_X^p$  is the penalty cost coefficient and  $P_X^{max}(t)$  is the maximum power for the intermittent resource  $X$ , at time  $t$ .

The third term in (6) is the reserve cost, obtained from the concept of overestimation of the intermittent resource [23, 27]. It represents the cost charged when the active power planned at an instant  $t$ , for the PVS or WGS, is greater than the available active power of these same systems, which is given by:

$$C_X^r(P_{Xd}(t), P_{Xp}(t)) = k_X^r \int_0^{P_{Xp}(t)} (P_{Xp}(t) - P_X(t)) f_{P_X}(P_X(t)) dP_X(t) \quad (9)$$

where  $k_X^r$  is the reserve cost coefficient.

### Diesel Generator Cost Model

The insertion of diesel generation systems (DGS) in microgrids aims to increase their self-sufficiency, since there is no way to guarantee the continuous supply of electricity from renewable sources. For most DGSs, a quadratic polynomial function satisfactorily represents the relationship between the generated power and the fuel consumption of the DGS [29]. The cost associated with the DGS is then given by:

$$F_{DG}(P_{DG}(t)) = C_f(aP_{DG}^2(t) + bP_{DG}(t) + c) \quad (10)$$

where  $P_{DG}(t)$  is the output power at time  $t$ ,  $C_f$  is the price of the consumed fuel, (\$/l) and  $a, b$  and  $c$  are cost coefficients.

### Battery Bank Cost Model

In this paper, the lifetime of the BB is optimized in the considered microgrid operation. This is done by modeling the cost of wear of the battery bank and the control of the state of charge (SOC), which represents, in percentage, the amount of charge existing in the BB.

Regarding the programming of the day-ahead operation in microgrids, the value of power flowing through the battery bank is determined by the generated active power and by the load demand at a given time  $t$ . The SOC at time  $t + 1$  is given by [9]:

$$SOC(t + 1) = SOC(t) - \alpha(P_{BB}(t) + (1 - \eta_b)|P_{BB}(t)|) \quad (11)$$

where  $SOC(t)$ ,  $P_{BB}(t)$  and  $\eta_b$  are the state of charge at time  $t$ , the power flowing through the battery bank, and the charging and discharging efficiency of the battery, respectively. Also,  $\alpha = \Delta t/E_{max}$ , with  $E_{max}$  being the nominal capacity of the BB (kWh), and  $\Delta t$  is the considered time interval.

The lifetime of the BB can be maximized in order to lead the battery bank to operating conditions that leads to the least possible wear [27]. This wear is mainly determined by the depth of discharge (DoD) to which the bank is subjected and by the number of cycles that the battery performs.

The cost of the charging and discharging process in a battery bank is associated to its degradation and a reduction in the lifetime of the same. The cost associated with operating the battery bank in the microgrid at each instant  $t$  is given by:

$$F_{BB}(P_{BB}(t)) = C_{bw} |P_{BB}(t)| \quad (12)$$

where  $C_{bw}$  is the BB's wear cost, which is directly related to the DoD  $\times$  Average Life Cycle curve, given by the battery manufacturer.

### PROPOSED FORMULATION FOR THE DAY-AHEAD OPERATIONAL PLANNING

The formulation proposed for the day-ahead operational planning is general enough to be applied in microgrids that operate in standalone mode and are constituted by short feeders, PVSSs, WGSs, DGSs, and storage systems based on BB. The DA-OP aims to determine the optimal day-ahead operational planning, in terms of active power dispatched by each generation unit and the supplied/absorbed power from the BB, considering the minimization of generation costs and optimization of the lifetime of the battery bank.

Considering only the active power programming of the energy resources, the proposed formulation is more suitable for microgrids with low consumption of reactive power or loads that operate close to the unitary power factor, which is the case of microgrids with a typical residential consumption profile. The DA-OP proposed in this paper is given by:

$$\min \sum_{t=1}^{24} \left[ \sum_{n=1}^{NPV} F_{PV}^n(P_{PVp}^n(t)) + \sum_{n=1}^{NWG} F_{WG}^n(P_{WGp}^n(t)) + \sum_{n=1}^{NDG} F_{DG}^n(P_{DG}^n(t)) + \sum_{n=1}^{NBB} F_{BB}^n(P_{BB}^n(t)) \right] \quad (13)$$

Subject to:

$$\sum_{n=1}^{NPV} P_{PVp}^n(t) + \sum_{n=1}^{NWG} P_{WGp}^n(t) + \sum_{n=1}^{NDG} P_{DG}^n(t) + \sum_{n=1}^{NBB} P_{BB}^n(t) - \sum_{n=1}^{NPD} P_D^n(t) = 0 \quad (14)$$

$$\underline{P_{PV}^n(t)} \leq P_{PVp}^n(t) \leq \overline{P_{PV}^n(t)} \quad (15)$$

$$\underline{P_{WG}^n(t)} \leq P_{WGp}^n(t) \leq \overline{P_{WG}^n(t)} \quad (16)$$

$$\underline{P_{DG}^n} \leq P_{DG}^n(t) \leq \overline{P_{DG}^n} \quad (17)$$

$$- \underline{P_{BB}^n(t)} \leq P_{BB}^n(t) \leq \overline{P_{BB}^n(t)} \quad (18)$$

$$(1 - \overline{DoD}) \leq SOC^n(t - 1) - \alpha(P_{BB}^n(t - 1) + (1 - \eta_b)|P_{BB}^n(t - 1)|) \leq 1 \quad (19)$$

where:

- $F_{PV}^n(P_{PVp}^n(t))$  represents the cost associated with the  $n$ -th PVS, of a total of  $N_{PV}$  PVSs and it is given by equation (7), assuming  $X = PV$ ;
- $F_{WG}^n(P_{WGp}^n(t))$  represents the cost associated with the  $n$ -th WGS, of a total of  $N_{WG}$  WGSs and it is given by equation (7), assuming  $X = WG$ ;
- $F_{DG}^n(P_{DG}^n(t))$  represents the cost associated with the  $n$ -th DGS, of a total of  $N_{DG}$  DGSs and it is given by equation (11);
- $F_{BB}^n(P_{BB}^n(t))$  represents the cost associated with the  $n$ -th BB, of a total of  $N_{BB}$  BB's and it is given by equation (13).
- $P_D^n$  represents the active power demanded for the  $n$ -th set of loads on the microgrid, at time  $t$ .

Also,  $\underline{P_{PV}^n(t)}$  and  $\overline{P_{PV}^n(t)}$ ,  $\underline{P_{WG}^n(t)}$  and  $\overline{P_{WG}^n(t)}$ ,  $\underline{P_{DG}^n}$  and  $\overline{P_{DG}^n}$  and  $\underline{P_{BB}^n(t)}$  and  $\overline{P_{BB}^n(t)}$  are the minimum and maximum power limits of the  $n$ -th PVS, WGS, DGS and BB, respectively.

In addition to the restrictions previously presented, it was considered that the initial SOC (in  $t = 1$ ) of the BB was equal to the final SOC (in  $t = 24$ ), after a full period of planning for the microgrid. Figure 2 briefly presents the step-by-step to solve the day-ahead operational planning in microgrids, that was applied in the test system presented in this paper.

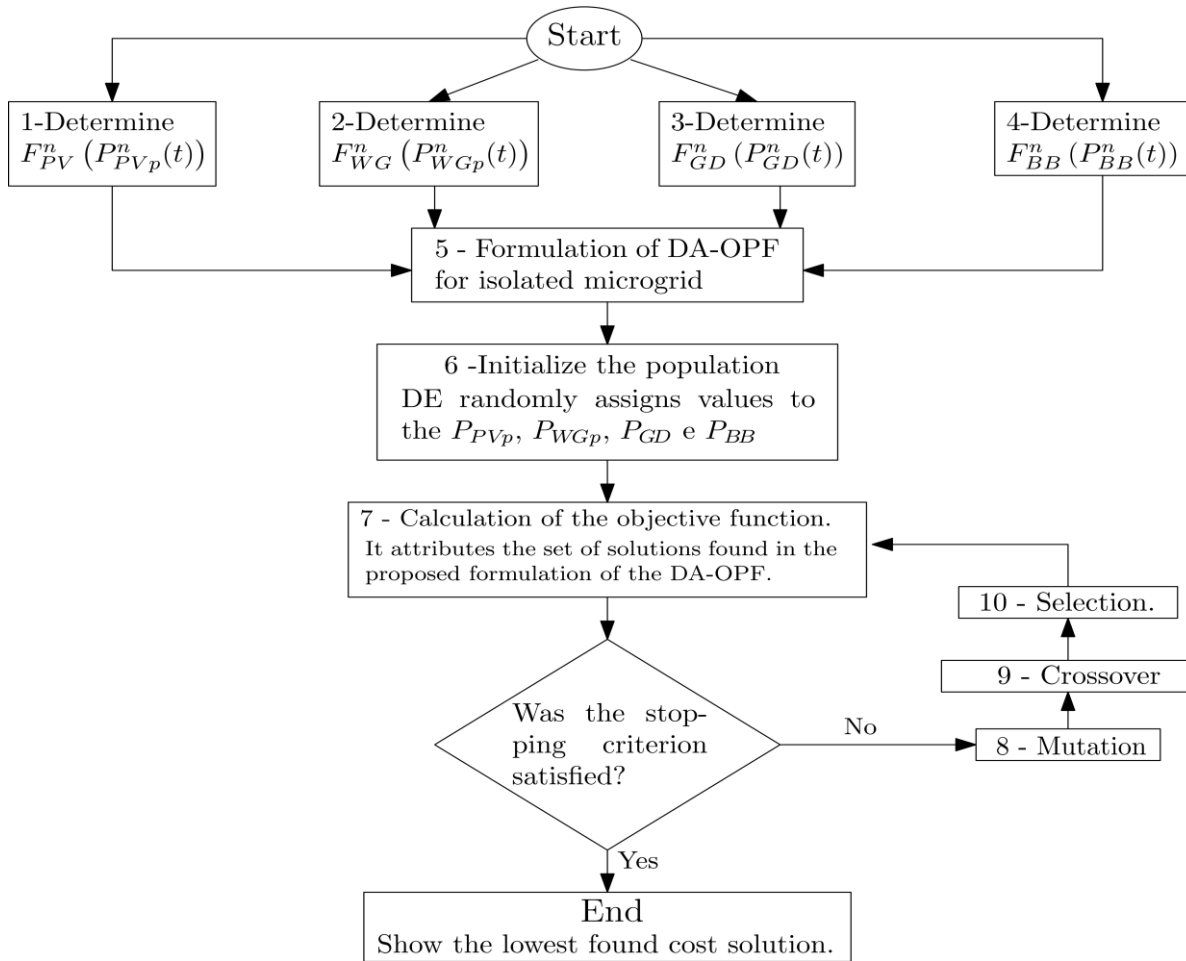


**Figure 2.** Flowchart of the developed algorithm.

Steps 1 and 2 show in Figure 2 consist of determining the probabilistic cost equation for the PVS and WGS, respectively. This is done by using the set of equations (6) - (9), assuming  $X = PV$  or  $X = WG$ . Steps 3 and 4 are dedicated to determining the cost functions associated with DGS and BB, respectively, by using equations (10) and (12). The set of parameters used for both systems can be found in Table 1.

In step 5 the optimization problem is formulated, using the set of equations (13) - (19), and finally, steps 6 to 10 are dedicated to the application of the differential evolution algorithm to the problem.

**Table 1.** Parameters used in the objective function.

| Parameter | $k_l^{pv}$ | $k_p^{pv}$ | $k_r^{pv}$ | $k_l^{wg}$ | $k_p^{wg}$ | $k_r^{wg}$ | $C_{bw}$ | $C_f$ | $a$   | $b$ | $c$ |
|-----------|------------|------------|------------|------------|------------|------------|----------|-------|-------|-----|-----|
| Value     | 0          | 6          | 8          | 0          | 4          | 3          | 0.065    | 1.2   | 0.246 | 0.1 | 0   |

## TESTS AND RESULTS

The operation schedule is discretized into 24 points, one for each hour of the day. For each operating point, the values that must be dispatched in terms of active power by the PVS, WGS and DGS, and the active power delivered or stored by the BB are obtained, that is, the power value  $P_k(t)$ , with  $k = \{PVp; WGp; DG; BB\}$ , and  $t = \{1; 2, \dots, 24\}$ .

To determine the most suitable DE configuration for the proposed problem, independent tests were performed varying the DE parameters as follows:

- The population size ( $N_p$ ) was varied in the range [20, 200] with a step of 20;
- The crossover constant ( $C_r$ ) was varied in the range of [0.1, 0.9] with a step of 0.1;
- The mutation Factor ( $F$ ) was varied in the range of [0.2, 1.8] with a step of 0.2.



All tests were performed for the  $DE/best/2/bin$  strategy, with a  $g_{max}$  equal to 10000 generations. The analysis criterion for choosing the parameters was the total cost of operating the microgrid. Considering the 810 possible combinations for the DE parameters, as previously described, the simulation results showed the configuration of parameters that presented the minimum cost for the proposed application is  $N_p = 140$ ,  $C_r = 0.9$ ,  $F = 0.4$ .

Figure 3 presents the isolated microgrid adopted as a test system to validate the proposed formulation of the DA-OP, whose technical information can be found in [27].

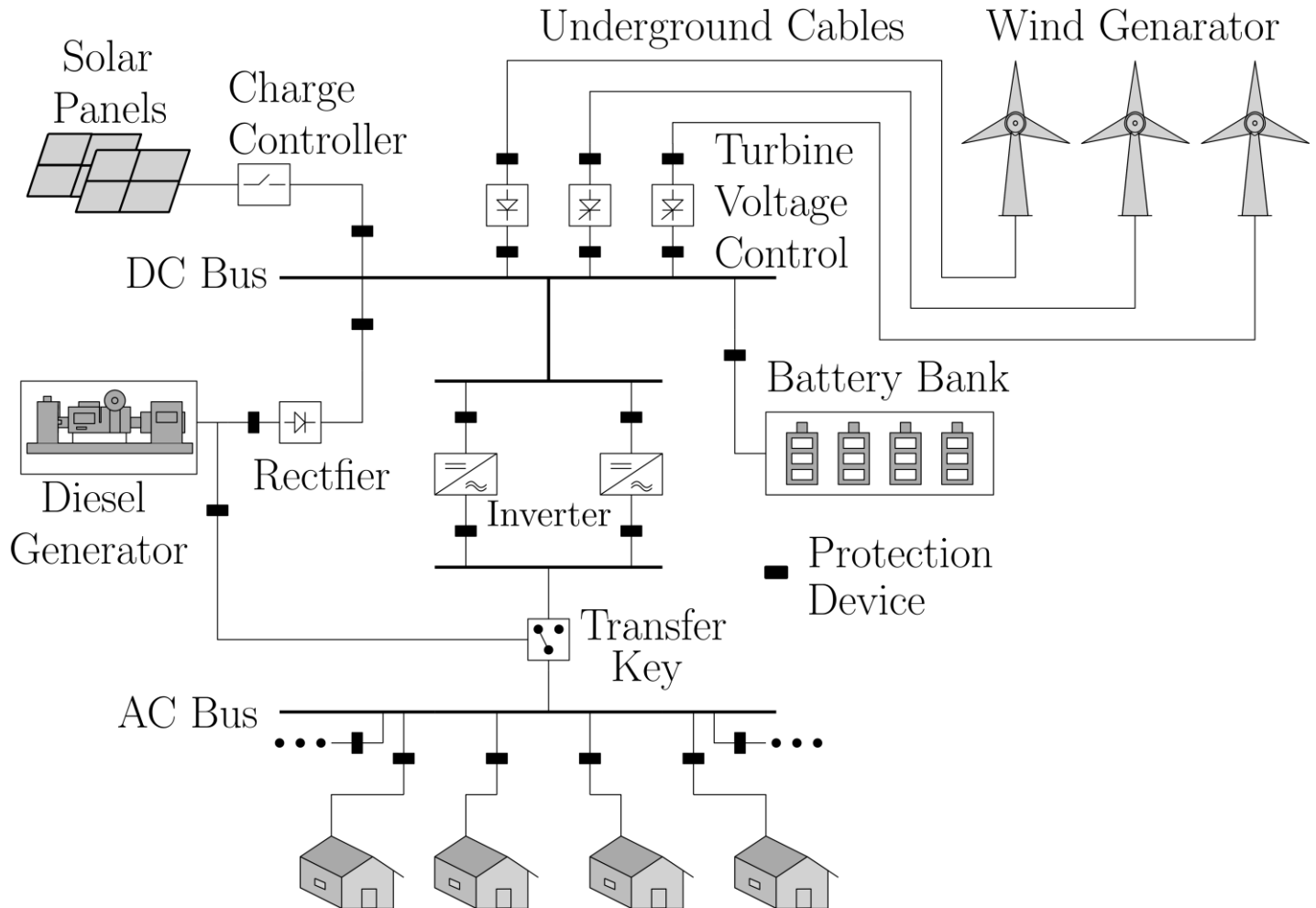


**Figure 3.** Test System - Lençóis Island Microgrid.

The microgrid presents a wind-solar generation system and it is located in the Lençóis Island, in the state of Maranhão, Brazil, and it has been operating since 2008, serving 24 hours a day a community with approximately 90 residences and more than 400 people. The  $\overline{P_{DG}^1}$ ,  $\overline{P_{PV}^1(t)}$  and  $\overline{P_{WG}^1(t)}$  values are 42 kW and 21 kW and 22.5 kW, respectively. The Battery Bank has 120 Lead-Acid batteries with an initial SOC of 0.75 and an  $E_{max}$  of 316.8 kWh. For this value of  $E_{max}$ ,  $\eta_b$  of 85% and  $\overline{DoD}$  of 50%, the maximum power that can be supplied in a time interval,  $\overline{P_{BB}^1(t)}$ , is 137.74 kW and the minimum,  $-\overline{P_{BB}^1(t)}$ , is -186.35 kW.

Also, this microgrid has a load profile as illustrated in Figure 4, short branches, with a voltage drop between generation and load lower than 0.3%. The loads are operating with a power factor close to 1.0 [30]. These characteristics allow the adoption of power flow equations comprising only the active power balance equations without considering active losses of the microgrid, without compromising the accuracy of the results obtained.

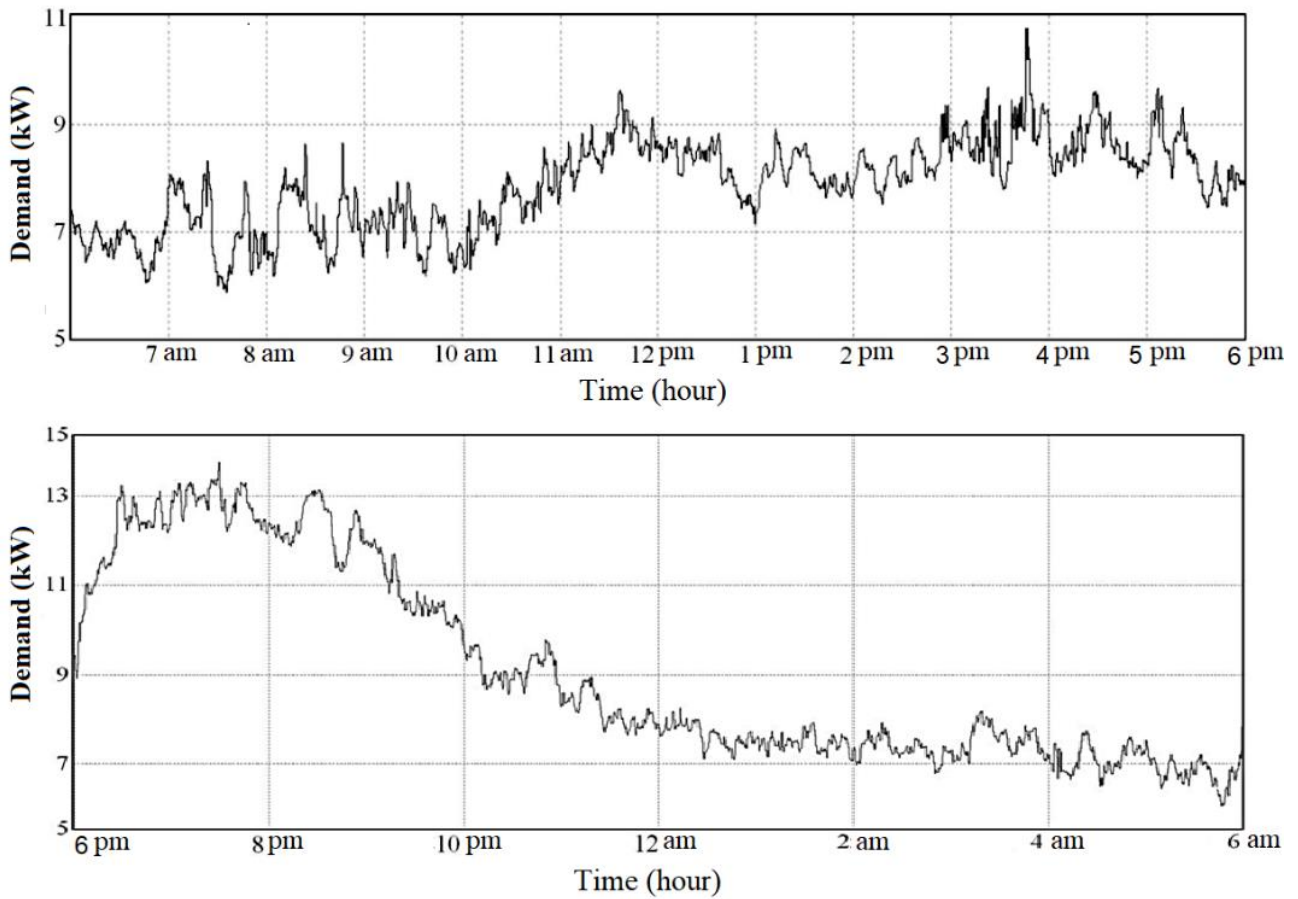


**Figure 4.** Demanded power of a typical day of the microgrid operation.

The input parameters of the proposed optimization are the solar radiation and wind speed pattern, which are estimated for the day under analysis, as well as the rated power of the generation for these resources, the state of charge, and maximum capacity of the battery bank, and load profile demanded by the microgrid. Technical parameters referring to the microgrid in Lençóis Island can be found in [27]. The climatic conditions referring to solar irradiance and average wind speed, for the day on which the microgrid operation is to be scheduled, were defined according to Table 2:

**Table 2.** Simulation scenarios performed.

| Scenario | Description                    | Characteristic                              | $k_{tu}$ | $V_m^{max} (m/s)$ |
|----------|--------------------------------|---|----------|-------------------|
| I        | Typical operating day          | PV - Normal<br>WG - Normal<br>Load - Normal | 0.864    | 12.4              |
| II       | Intermediate partly cloudy day | PV - Medium<br>WG - Medium<br>Load - Normal | 0.432    | 10.4              |
| III      | Critical day: cloudy/rainy     | PV - Low<br>WG - Low<br>Carga - Normal      | 0.216    | 8.4               |

It is important to emphasize that for all the proposed scenarios, the installed power capacity of the PVS and WGS are equal to 21 kW and 22.5 kW, respectively. However, the maximum available power of each hour, for both PVS and WGS, is a variable that depends on weather conditions that change throughout the day. Therefore, the limits for  $P_{PVp}(t)$  and  $P_{WGP}(t)$  are determined by their respective probability density functions,  $f_{PV}(P_{PVp}(t))$  and  $f_{WG}(P_{WGP}(t))$ , where it is possible to obtain the probability of occurrence and the maximum and minimum limits for the active power generated through the intermittent sources for each hour of the day.

Figure 5 exemplifies a typical PDF for an hour interval,  $t$ , showing the points on the curve where the maximum and minimum power limits are determined for both intermittent sources.

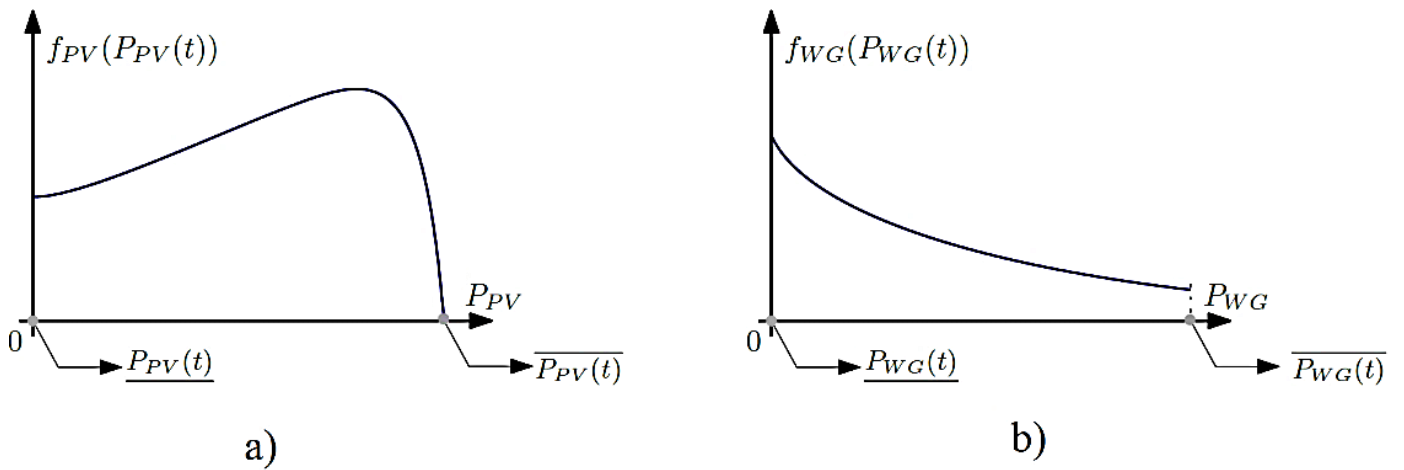


**Figure 5.** PDF example for the active output power of the sources intermittent.

**Scenario I**

As described in Table 2, Scenario I represents a day when the climatic conditions are ideal for generation from PVS and WGS. The probability density functions of the PVS and WGS are shown in Figures 6 and 7, respectively, throughout the day.

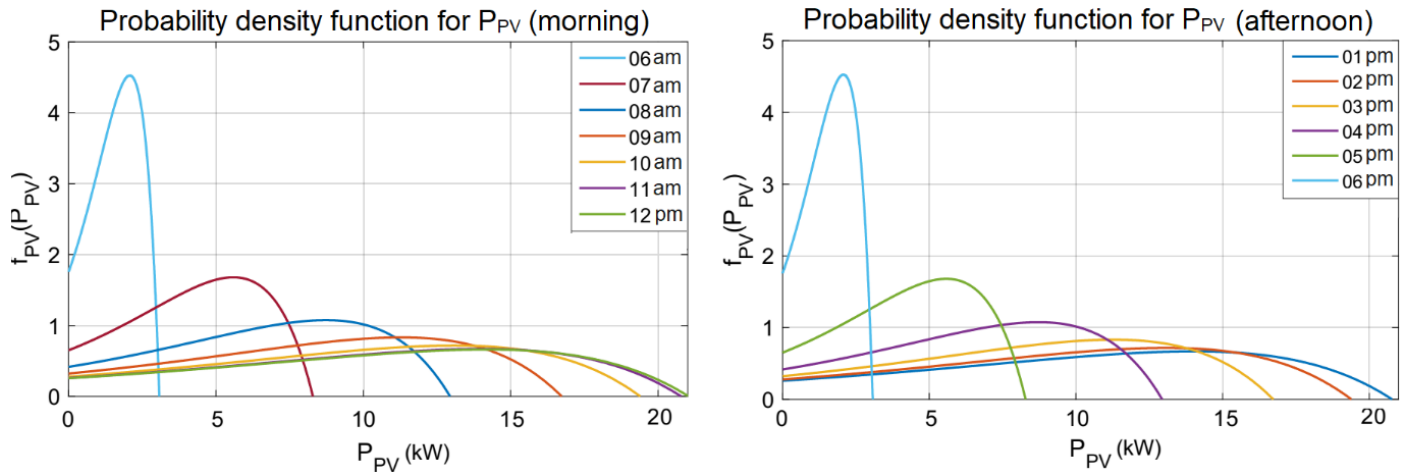


**Figure 6.** PDF for  $P_{PV}(t)$  in scenario I.

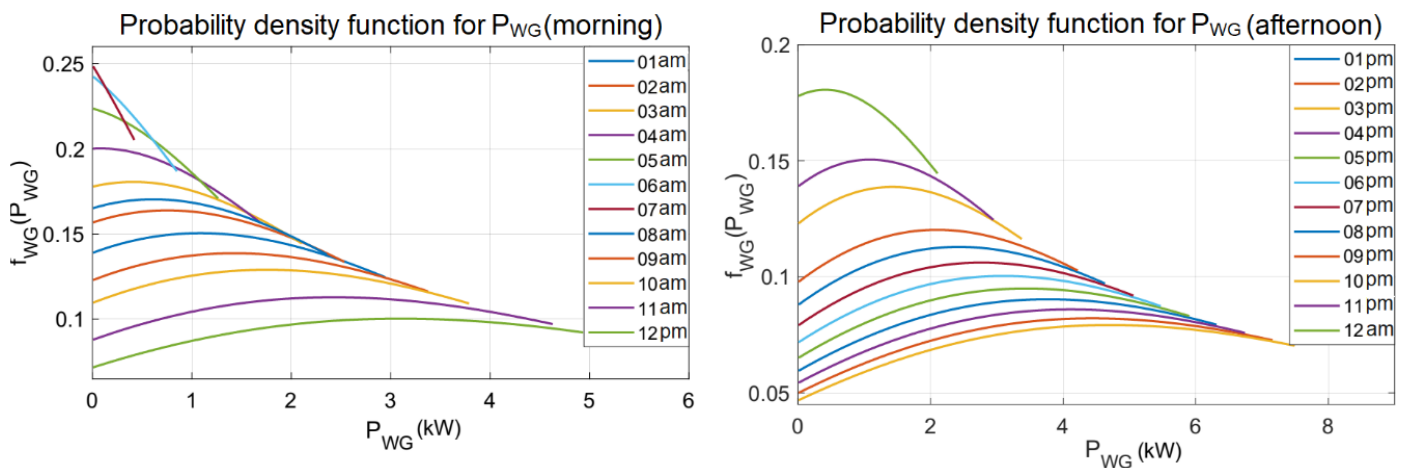


**Figure 7.** PDF for  $P_{WG}(t)$  in scenario.

Using the PDF shown in Figures 6 and 7 and the other input parameters of the test system, steps 5 to 10 of the proposed step-by-step to solve the day-ahead programming were performed. The obtained day-ahead operational planning of the microgrid in Lençóis Island is shown in Figure 8.

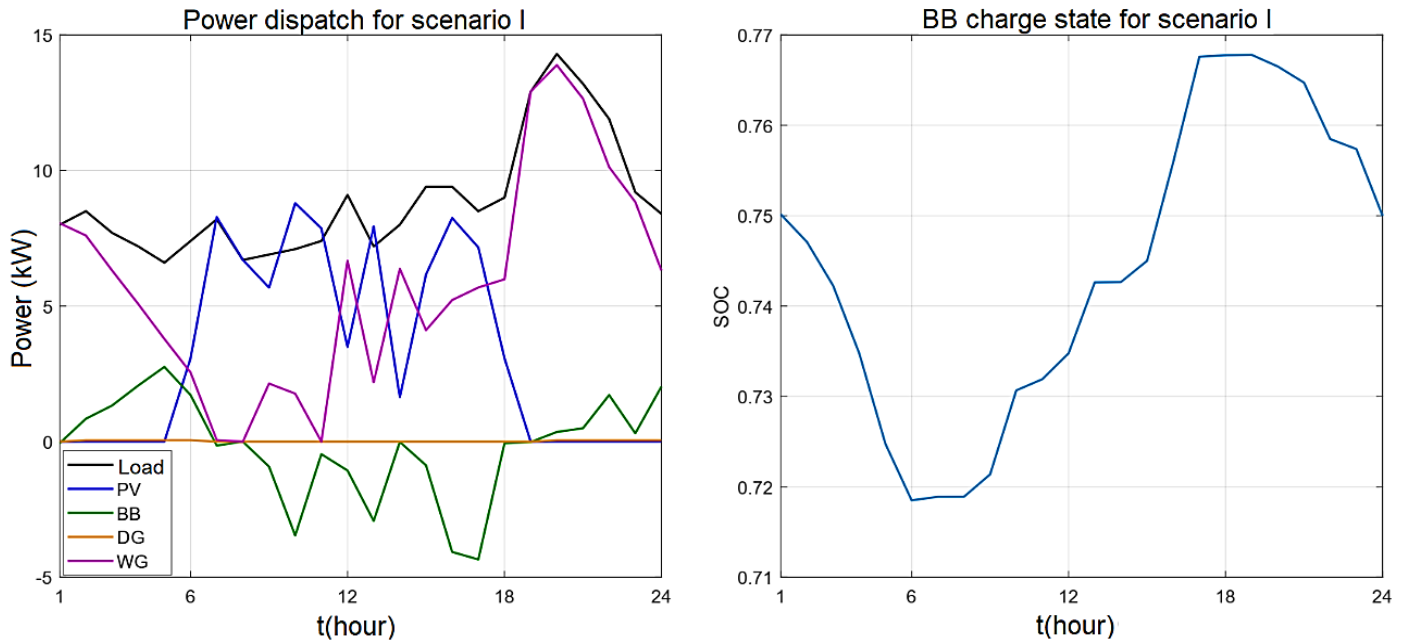


**Figure 8.** Power dispatch and state of charge obtained for Scenario I.

From the results obtained for scenario I, it is observed the power dispatch values obtained guarantee that the load demand is met at all 24 operating points. Furthermore, at each hour interval, the battery bank's state of charge remains within the specified limits, which contributes to less degradation of the battery bank, optimizing its useful life.

It is worth pointing out that the battery bank supplies energy to the load only in intervals where the power that could be generated by intermittent sources is lower than the demand of the load to be served in that interval. Even so, by the end of the day, the state of charge of the battery bank was equal to the stipulated value, guaranteeing the same operational conditions for each day of microgrid operation. Due to the favorable climatic conditions for generation through intermittent resources in this scenario, diesel generation is not used, avoiding unnecessary fuel consumption. In other words, intermittent sources were prioritized to make up the energy dispatch obtained because they present lower operating costs than the battery bank and the diesel generation system.

Comparing the active output powers provided by intermittent resources, the applied optimization technique prioritized the use of the PVS to compose the dispatch, especially at times when the probability of generating energy from the WGS was low, compared to its nominal power (intervals 7 to 11). On the other hand, the use of WGS is prioritized to compose the energy dispatch when PVS generation was not available (intervals 1 to 6 and 18 to 24).

## Scenario II

As described in Table 2, Scenario II represents a day where the hourly clearness index and wind speed reach maximum values, in each hour interval, lower than those reached in Scenario I. The probability density functions of the PVS and WGS are shown in Figures 9 and 10, respectively, throughout the day.

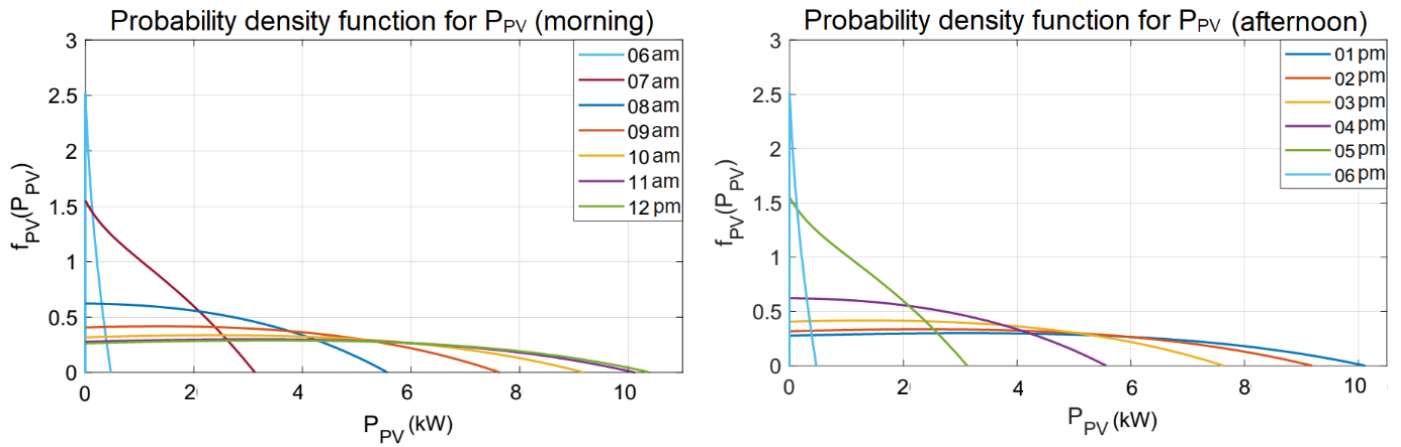


Figure 9. PDF for  $P_{PV}(t)$  in scenario II.

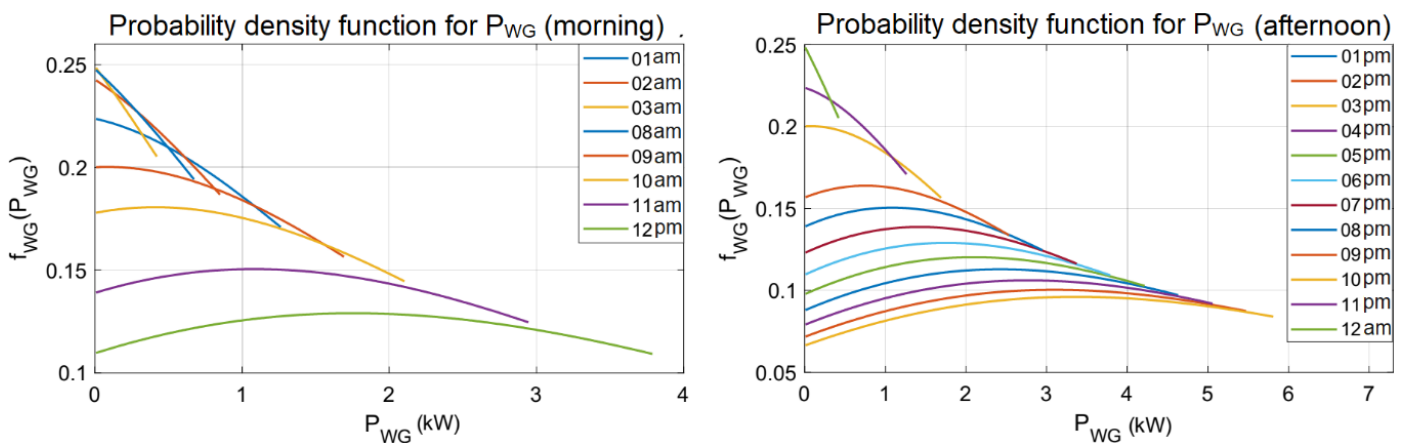


Figure 10. PDF for  $P_{WG}(t)$  in scenario II.

Using the PDF shown in Figures 9 and 10 and the other input parameters of the test system, steps 5 to 10 of the proposed step-by-step to solve the day-ahead programming were performed. The obtained day-ahead operational planning of the microgrid in Lençóis Island, for scenario II, is shown in Figure 11.

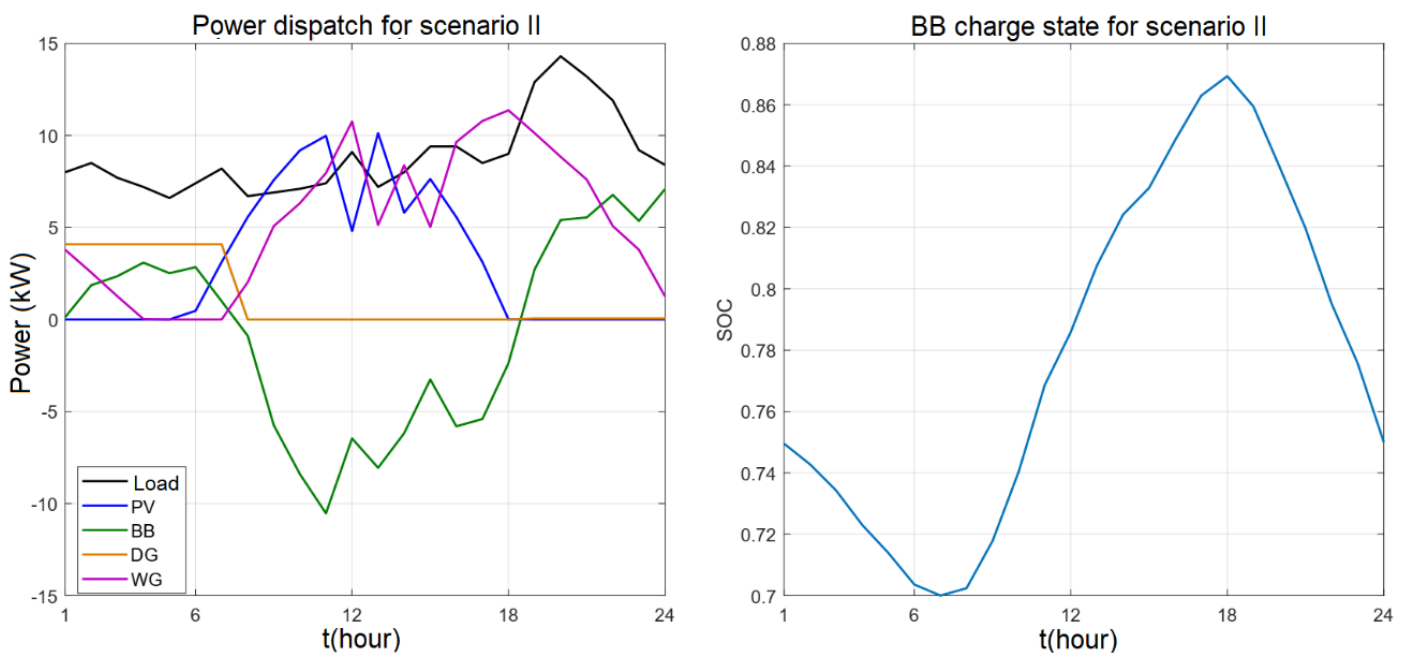


Figure 11. Power dispatch and state of charge obtained for Scenario II.

In scenario II, the power dispatch values guarantee the load demand is met at all 24 operating points and the state of charge of the battery bank is maintained within the specified limits, in a similar way to what was obtained in scenario I. Other similar behaviors between the two scenarios were the supply of energy by the battery bank only at intervals in which the intermittent sources were unable to meet the demand and the fact the state of charge was equal to the stipulated value by the end of the day.

Different from the results obtained for scenario I, the diesel generator provided power to the microgrid in the first hours of the day, due to the climatic conditions for power generation through intermittent resources and a greater use of the battery bank occurred. These facts lead to a higher cost of operating the microgrid in this scenario.

**Scenario III**

Scenario III, as described in Table 2 represents a day where the probabilities of generating power from the PVS and WGS are extremely low compared to scenarios I and II. The probability density functions of the PVS and WGS are shown in Figures 12 and 13, respectively, throughout the day.

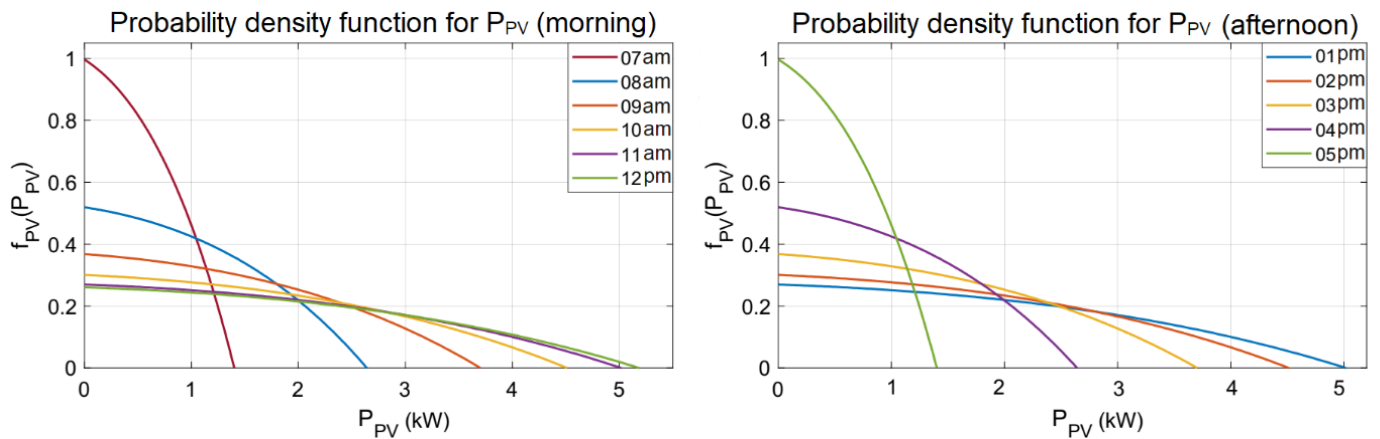


**Figure 12.** PDF for P<sub>PV</sub>(t) in scenario III.

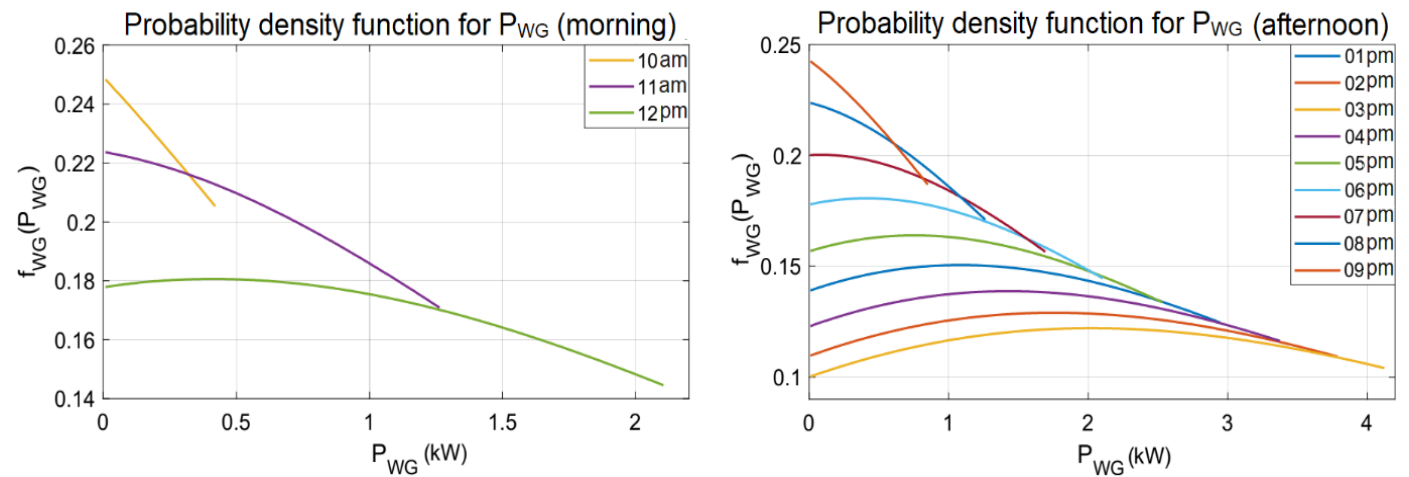


**Figure 13.** PDF for P<sub>WG</sub>(t) in scenario III.

Using the PDF shown in Figures. 12 and 13 and the other input parameters of the test system, the steps 5 to 10 of the proposed step-by-step to solve the day-ahead programming of the microgrid in Lençóis Island were performed. The obtained day-ahead operational planning for the scenario III is shown in Figure 14.

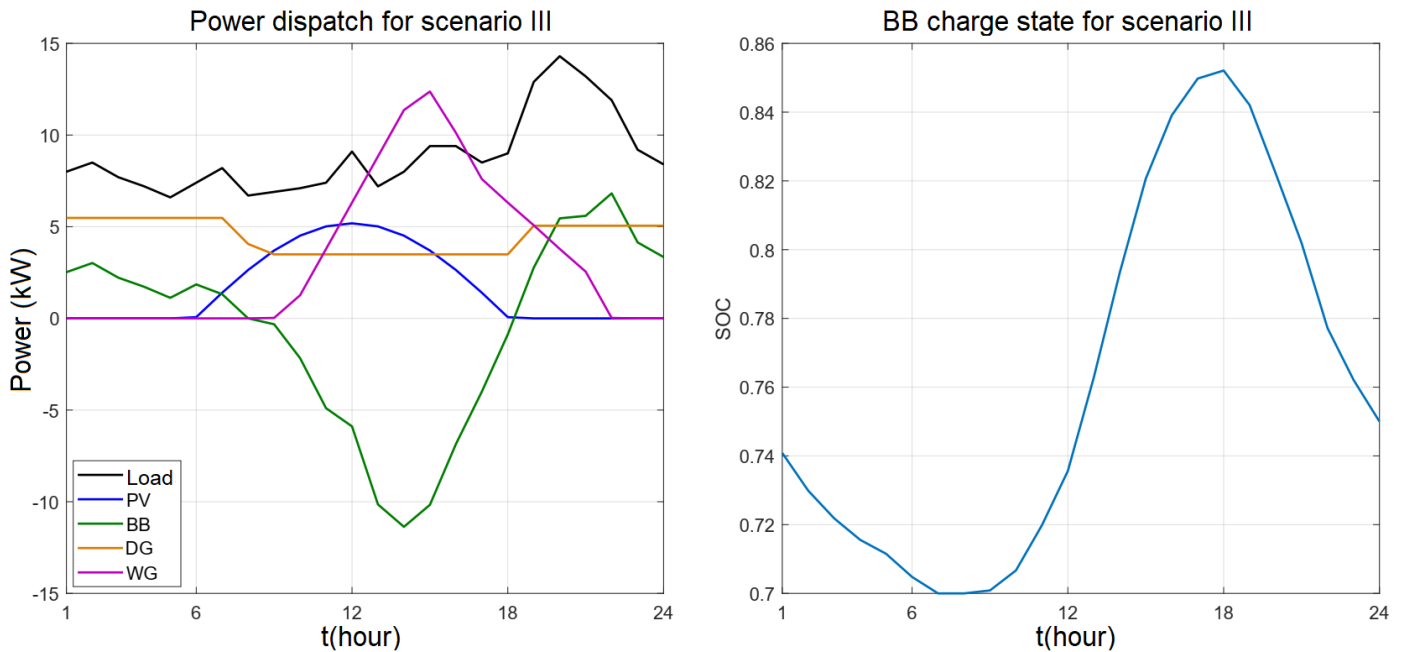


**Figure 14.** Power dispatch and state of charge obtained for Scenario III.

Once the climatic conditions for power generation through intermittent resources are not for favorable in scenario III, it can be concluded from Figure 14 that the diesel generator was used throughout the day. Besides that, the battery bank is charged at intervals when energy generation from intermittent resources reaches higher values.

Compared to scenarios I and II, the use of the battery bank is significantly higher in this scenario, since energy generation from intermittent sources presents very low values, compared to their nominal generation capacities. This fact, added to the greater use of the diesel generator, promotes an operation that presents higher costs.

It is important to emphasize the results shown in Figures. 7, 10, and 13 are the ones with the lowest cost of a total of 50 simulations performed for each of the scenarios. The obtained cost values and the average simulation times for each of the scenarios are shown in Table 3. All the tests were performed by a computer equipped with an Intel Core i5 processor and 8 GB of RAM.

**Table 3.** Costs and simulation time for scenarios I, II and III.

| Scenario | Minimum Cost (\$) | Average Cost (\$) | Maximum Cost (\$) | Standard deviation | Average time of Simulations (s) |
|----------|-------------------|-------------------|-------------------|--------------------|---------------------------------|
| I        | 4.65              | 5.10              | 10.66             | 1.40               | 1425                            |
| II       | 47.816            | 48.126            | 48.33             | 0.16               | 1789                            |
| III      | 169.27            | 169.27            | 169.27            | 0.01               | 1527                            |

As it can be seen in Table 3, in scenarios where the generation of power from the PVS and the WGS is low, the costs tend to be higher, compared to scenarios where the generation of these intermittent resources is high. A reason for that is the proposed formulation incorporates climatic conditions associated with the PVS and WGS in the cost function model, through their respective probability density functions.

Another factor that influences the increase of costs in scenarios with a reduced availability of renewable generation is the need to use the auxiliary resources of the microgrid to compose the power dispatch as the generation of PVS and WGS is restricted in scenarios II and III.

It is also possible to observe in scenarios where intermittent sources have less availability, there is less variability in the solutions found by the optimization technique, leading to a lower standard deviation of the cost. This occurs because the reduction in generation from intermittent sources reduces the search space, making the technique find solutions more concentrated at optimal points.

## CONCLUSIONS

The purpose of this paper was to apply a probabilistic cost model in the day-ahead planning of microgrids in standalone operation mode. Most approaches that deal with the intermittent nature of solar photovoltaic and wind generation systems in a day-ahead planning ignore important issues in the operation of microgrids, such as optimization of the lifetime of storage systems. For this reason, a new day-ahead operational planning methodology was proposed by considering in the objective function the intermittency related to the output power of the renewable generation, as well as the costs of the battery bank degradation and conventional diesel generator.

The results were performed in a microgrid located in the Lençóis Island, Brazil, and show that the adoption of a stochastic approach for the intermittent sources makes day-ahead planning in microgrids sensitive to the climatic conditions that characterize each proposed scenario. Furthermore, by considering the costs associated with battery bank degradation in the formulation of the problem, the long-term costs of operating the microgrid tend to be reduced.

## Future Works

The next steps of this research are:

- To adopt a non-ideal optimal power flow model in order to make the energy planning tool more embracing;
- To assign other operational aspects associated with battery banks, for example, limits of charge and discharge that can occur in an operating range;
- Using the energy planning obtained via DA-OP as an initial starting point for the formulation of an RT-PD.

**Funding:** This research received no external funding.

**Acknowledgments:** The authors acknowledge the financial support of the Coordenação de Aperfeiçoamento de Pessoal de Nível Superior—Brasil (CAPES).

**Conflicts of Interest:** The authors declare no conflict of interest.

## REFERENCES

1. Lasseter RH. Microgrids. In: IEEE. 2002 IEEE Power Engineering Society Winter Meeting. Conf. Proc. (Cat. No. 02CH37309). [S.l.], 2002. v. 1, p. 305–8.
2. Oubbati Y, Arif, S. Transient stability constrained optimal power flow using teaching learning based optimization. In: IEEE. 2016 8th Int. Conf. Modelling, Identif. Control (ICMIC). [S.l.], 2016. p. 284–9.
3. Reddy SS, Bijwe P. Day-ahead and real time optimal power flow considering renewable energy resources. *Int. J. Electr. Power Energy Syst.*, Elsevier, v. 82, p. 400–8, 2016.
4. Liu Y, Qu Z, Xin H, Gan D. Distributed real-time optimal power flow control in smart grid. *IEEE Trans. Power Syst.* 2026;32(5):3403–14.
5. Tang Y, Dvijotham K, Low S. Real-time optimal power flow. *IEEE Trans. Smart Grid.* 2017;8(6):2963–73.
6. Arnold M, Andersson G. Model predictive control of energy storage including uncertain forecasts. In: CITESEER. *Power Syst. Comput. Conf. (PSCC)*, Stockholm, Sweden. [S.l.], 2011;23:24–9.
7. Biswas PP, Suganthan P, Amaratunga GA. Optimal power flow solutions incorporating stochastic wind and solar power. *Energy Convers. Manag.*, Elsevier, 2017;148:1194–207.
8. Riffonneau Y, Bacha S, Barruel F, Ploix S. Optimal power flow management for grid connected pv systems with batteries. *IEEE Trans. Sustain. Energy.* 2011;2(3):309–20.
9. Tazvinga H, Zhu B, Xia X. Optimal power flow management for distributed energy resources with batteries. *Energy Convers. Manag.*, Elsevier. 2015;102:104–10.
10. Wen X, Abbes D, Francois B. Stochastic optimization for security-constrained day-ahead operational planning under pv production uncertainties: Reduction analysis of operating economic costs and carbon emissions. *IEEE Access*, 2021;9:97039–52
11. Filho MOL, Pinto RS, Campos AC, Vila CU, Tabarro FH. Day-ahead robust operation planning of microgrids under uncertainties considering DERs and demand response. In: IEEE. 2021 IEEE PES Innovative Smart Grid Technol. Conf.-Latin America (ISGT Latin America). IEEE, 2021.
12. Souza WFS, Oliveira AER, Kuiava R, Leandro GV, Rodrigues LFM. Stochastic optimal power flow applied in day-ahead planning of isolated microgrids. In: IEEE. 2020 IEEE Power & Energy Soc. Gen. Meet. (PESGM). IEEE, 2020;1-5.
13. Souza WFS, Oliveira AER, Kuiava R, Leandro GV. [Optimal Power Flow Applied to Day-Ahead Planning of Isolated Microgrids]. In: *Simpósio Bras. Sist. Elétricos (SBSE)*. v. 1, n. 1, 2020.



14. Hossain E, Kabalci E, Bayindir R, Perez R. Microgrid testbeds around the world: State of art. *Energy Convers. Manag.*, Elsevier, 2014;86:132–53.
15. Sun J, Hu C, Liu L, Chen M, Xiang Y, Shi J. Day-ahead economic optimal operation plan based real-time dispatch for power grid with high proportion of new energies. In: IEEE. 2021 IEEE 2nd China Int. Youth Conf. Electr. Eng. (CIYCEE). IEEE, 2021.
16. Price K, Storn RM, Lampinen JA. *Differential evolution: a practical approach to global optimization*. [S.l.]: Springer Sci. Bus. Media, 2006.
17. Orgill J, Hollands K. Correlation equation for hourly diffuse radiation on a horizontal surface. *Sol. Energy*, Elsevier, 1977;19(4):357–59.
18. Erbs D, Klein S, Duffie J. Estimation of the diffuse radiation fraction for hourly, daily and monthly-average global radiation. *Sol. Energy*, Elsevier. 1982;28(4):293–302.
19. Tina G, Gagliano S. Probabilistic analysis of weather data for a hybrid solar/wind energy system. *Int. J. Energy Res.*, Wiley Online Library. 2011;35(3):221–32.
20. Tina G, Gagliano S, Raiti S. Hybrid solar/wind power system probabilistic modelling for long-term performance assessment. *Sol. Energy*, Elsevier. 2006;80(5):578–88.
21. Pillai SU, Papoulis A. *Probability, random variables, and stochastic processes*. [S.l.]: McGraw-Hill Times Roman by Sci. Typogr, 2002. v. 2.
22. Justus C, Hargraves W, Mikhail, A, Graber D. Methods for estimating wind speed frequency distributions. *J. Appl. Meteorol.* 1978;17(3):350–53,
23. Hetzer J, David CY, Bhattarai K. An economic dispatch model incorporating wind power. *IEEE Trans. Energy Convers.* 2008;23(2):603–11.
24. Stevens M, Smulders P. The estimation of the parameters of the weibull wind speed distribution for wind energy utilization purposes. *Wind Eng.*, JSTOR, 1979. p. 132–45.
25. Abedini M, Moradi MH, Hosseinian SM. Optimal management of microgrids including renewable energy sources using gпсо-gm algorithm. *Renew. Energy*, Elsevier, 2016;90:430–39.
26. Yang H, Wei Z, Chengzhi L. Optimal design and techno-economic analysis of a hybrid solar–wind power generation system. *Appl. Energy*, Elsevier. 2009;86(2):163–9.
27. Souza WFS. [Day-Ahead Planning of Isolated Microgrids]. [dissertation]. Federal University of Paraná, 2020.138 p.
28. Eldesouky AA. Security and stochastic economic dispatch of power system including wind and solar resources with environmental consideration. *Int. J. Renew. Energy Res. (IJRER)*. 2013;3(4):951–58.
29. Wood AJ, Wollenberg BF, Sheblé GB. *Power generation, operation, and control*. John Wiley & Sons, 2013.
30. Matos JGD. [Power control in isolated microgrids with wind turbines and distributed battery banks]. [Dissertation] Federal University of Maranhão, 2014.115 p.



© 2024 by the authors. Submitted for possible open access publication under the terms and conditions of the Creative Commons Attribution (CC BY) license (<https://creativecommons.org/licenses/by/4.0/>)